HHS Public Access

Author manuscript

*Int J Radiat Oncol Biol Phys*. Author manuscript; available in PMC 2016 December 08.

Published in final edited form as:

*Int J Radiat Oncol Biol Phys*. 2015 September 01; 93(1): 64–71. doi:10.1016/j.ijrobp.2015.05.017.

# EFFECTS OF SURGERY AND PROTON THERAPY ON CEREBRAL WHITE MATTER OF CRANIOPHARYNGIOMA PATIENTS

**Jinsoo Uh, PhD**[*], **Thomas E. Merchant, DO, PhD**[*], **Yimei Li, PhD**[†], **Xingyu Li, MS**[†], **Noah D. Sabin, MD**[*], **Daniel J. Indelicato, MD**[‡], **Robert J. Ogg, PhD**[*], **Frederick A. Boop, MD**[§], **John A. Jane Jr., MD**[||], and **Chiaho Hua, PhD.**[*]

[*]Department of Radiological Sciences, St. Jude Children's Research Hospital, Memphis, TN, USA

[†]Department of Biostatistics, St. Jude Children's Research Hospital, Memphis, TN, USA

[‡]Department of Radiation Oncology, University of Florida, Jacksonville, FL, USA

[§]Semmes-Murphey Neurologic and Spine Institute, Memphis, TN, USA

[||]Department of Neurosurgery, University of Virginia, Charlottesville, VA, USA

## Abstract

**Purpose—**To determine the radiation dose-effect on the structural integrity of cerebral white matter in craniopharyngioma patients receiving surgery and proton therapy.

**Methods and Materials—**Fifty-one patients (aged 2.1–19.3 years) with craniopharyngioma underwent surgery and proton therapy in a prospective therapeutic trial. Anatomical magnetic resonance images acquired after surgery but before proton therapy were inspected to identify white matter structures intersected by surgical corridors and catheter tracks. Longitudinal diffusion tensor imaging (DTI) was performed to measure microstructural integrity changes in cerebral white matter. Fractional anisotropy (FA) derived from DTI was statistically analyzed for 51 atlas-based white matter structures of the brain to determine radiation dose-effect. FA in surgery-affected regions in the corpus callosum was compared to that in its intact counterpart to determine whether surgical defects affect radiation dose-effect.

**Results—**Surgical defects were seen most frequently in the corpus callosum because of transcallosal resection of tumors and insertion of ventricular or cyst catheters. The longitudinal DTI data indicated reductions in FA 3 months after therapy, which was followed by a recovery in most white matter structures. A greater FA reduction was correlated with a higher radiation dose in 20 white matter structures, indicating a radiation dose-effect. The average FA in the surgery-

Corresponding author: Jinsoo Uh, Ph.D., Department of Radiological Sciences, Mail Stop 220, St. Jude Children's Research Hospital, 262 Danny Thomas Place, Memphis, TN 38105-3678. Tel: (901) 595-6545; Fax: (901) 595-3981; jinsoo.uh@stjude.org.

Parts of this paper have been presented at the 2014 ASTRO's 56th annual meeting in San Francisco, CA, USA.

Conflicts of Interest Notification: No actual or potential conflicts of interest exist.

affected regions before proton therapy was smaller ($P$ =0.0001) than that in their non-surgery affected counterparts with more intensified subsequent reduction of FA ($P$=0.0083) after therapy, suggesting that surgery accentuated the radiation dose-effect.

**Conclusions—**DTI data suggest that mild radiation dose-effects occur in patients with craniopharyngioma receiving surgery and proton therapy. Surgical defects present at the time of proton therapy appear to accentuate the radiation dose-effect longitudinally. This study supports consideration of pre-existing surgical defects and their locations in proton therapy planning and studies of treatment effect.

**Keywords**

craniopharyngioma; proton therapy; diffusion tensor imaging (DTI); corpus callosum

## Introduction

Childhood craniopharyngioma is a histologically benign but locally aggressive intracranial tumor typically arising in the suprasellar region. Because of the sensitive location of the tumor, limited surgical resection followed by radiation therapy is often the treatment approach of choice (1, 2). Despite successful disease control, efforts are still ongoing, particularly in radiation therapy, to minimize treatment-related long-term effects by reducing the radiation dose to non-targeted areas. Conformal radiation therapy has been commonly used (3), and proton therapy trials are now being conducted (4, 5).

The ability to assess radiation effects on normal brain tissues after treatment would provide valuable information in optimizing radiation therapy techniques. Diffusion tensor imaging (DTI) is a magnetic resonance imaging (MRI) modality suitable for this purpose because of its superior sensitivity to microstructural integrity in cerebral white matter, which is generally more prone to radiation-induced injury than is cortical gray matter (6). Radiation-induced injury in childhood cancer survivors causes DTI-derived indices that are altered from those of healthy controls (7, 8). Longitudinal studies in adult brain tumor patients have shown dose-dependent acute and subacute changes in DTI indices after therapy (9). Such early response to irradiation may be useful for predicting subsequent progression that may vary individually (10). Several studies have reported correlation between changes in DTI indices and decreased neurocognitive functionality such as intelligence quotient scores and processing speeds (11–14), suggesting DTI as a potential imaging biomarker for treatment-related neurotoxicity. A notable finding in these studies is that radiation dose-effect is fiber tract- or region-dependent (15–18). If an association with observed neurotoxicity can be established, then knowledge of differential radiation sensitivity would be valuable in treatment planning to protect more vulnerable brain regions.

In this study, we used DTI to assess structural integrity of white mater in patients with craniopharyngioma who received surgery and proton therapy. While our long-term goal is to identify white matter regions at higher risk for neurotoxicity, we currently aim to determine the radiation dose-effect on white matter integrity using DTI-derived fractional anisotropy (FA) as a surrogate marker. This aim is original because DTI has rarely been used for evaluation of craniopharyngioma patients receiving radiation therapy. An additional novel

aim in this study is to determine whether surgical defects accentuate the radiation dose-effect, which has not been considered in previous DTI studies.

## Methods and Materials

### Patients and treatment

A total of 56 patients with craniopharyngioma were enrolled in an ongoing institutional proton therapy trial between August 2011 and April 2014. Five of the enrolled patients were excluded from analysis because of severe metallic artifact in MR images and unavailability of DTI data. Among the 51 analyzed patients (29, female), the median age at the initiation of proton therapy was 9.2 years (range 2.1–19.3 years). The therapeutic trial incorporating the present imaging study was approved by the Institutional Review Board.

Patients underwent subtotal tumor resection and other surgical procedures for cyst decompression and ventricular drainage. They received proton therapy with the double-scattering technique, which typically included 3 fields: a right-superior-anterior-oblique beam, a left-superior-anterior-oblique beam, and a vertex beam. The total prescribed dose was 54 Cobalt Gray Equivalent (CGE) to the planning target volume, given in 1.8 CGE per fraction per day, 5 days per week, for a period of 6 weeks. The median time from tumor surgery to the start of proton therapy was 97 days (range, 16 days to 3.8 years).

### Acquisition and processing of DTI data

DTI data were acquired at baseline before proton therapy, every 3 months for the first year, and every 6 months thereafter. Median time from baseline to the most recent DTI was 12 months (range, 0–36 months). DTI scans were performed on a 1.5T MR scanner (Avanto; Siemens Medical Solutions, Enlargen, Germany) with typical image acquisition parameters detailed elsewhere (18). The DTI data were processed by using FSL (FMRIB, Oxford, UK) to derive FA maps.

### Atlas-based regions of interest

We used a set of white matter regions of interest (ROIs) defined by the International Consortium of Brain Mapping (ICBM) DTI-81 white matter atlas (19) to facilitate classifying structures affected by surgery and determine the radiation dose-effect in each region. The body of the corpus callosum was further parcellated into rostral body, anterior midbody, posterior midbody, and isthmus (20), resulting in 51 total number of ROIs in a standard brain space (MNI152).

### Skeleton-based mean of FA and dose

For the statistical analysis, mean values of FA and dose for each of the atlas-based ROIs were computed. We used the “skeleton-based mean” (21), which averages only FA or dose values projected onto pre-defined “white matter skeletons” (22) instead of all voxels in an ROI, to mitigate the effects of partial volume and mis-registration between individual brain and the ROIs in the standard brain.

### Identification of white matter structures affected by surgery

We visually inspected T1-weighted MR images at baseline to locate apparent surgical corridors or catheter tracks. The atlas-based ROIs in the standard space were inversely transformed onto the individual MR images to identify white matter structures corresponding to the surgical defects.

### Determination of the effects of radiation and surgery

The radiation dose-effect in each of the atlas-based ROIs was statistically tested by using a piece-wise linear mixed-effect model (LMEM) on the skeleton-based mean values of dose and longitudinal FA. This model accounted for normal age-related effect and transition of FA trend from reduction to recovery.

We tested whether a pre-existing surgical defect affects the radiation dose-effect, focusing on the corpus callosum for the following reasons: 1) It is the largest white matter structure in the human brain and is thereby less prone than other structures to confounding effects in DTI (e.g., partial volume effect); 2) The radiation effect on this structure has been extensively studied using DTI (9, 15); and 3) The corpus callosum in patients with craniopharyngioma tends to be affected by surgery and to receive relatively high doses from proton therapy. For this statistical test, the patients were categorized into two groups: those with surgical defects in the corpus callosum (n=17, “test group”) and those without them (n=34, “control group”). We defined “surgery-affected ROIs” in the corpus callosum for the test group and their counterpart ROIs for the control group besides previously defined atlas-based ROIs to take into account varying locations of the surgical defects in individuals (Fig. 1). Then, baseline and longitudinal FA values in these ROIs of the two groups were compared by using a linear regression model and a LMEM model, respectively.

Additional comparisons between the test and control groups were made to evaluate confounding effects due to characteristic differences between these groups that could cause global differences in FA. We compared baseline and longitudinal FA values in white matter structures not affected by surgery.

Statistical analyses were performed by using SAS software, version 9.3 (SAS Institute Inc., Cary, NC, USA). A *P*-value less than 0.05 was considered to be statistically significant after false-discovery rate control was used to correct for multiple comparisons.

## Results

### Locations of surgical defects in white matter

Surgical corridors or catheter tracts were seen in 16 white matter structures on MR images (Table 1). Among bilateral structures, the right-sided regions tended to be more affected by surgery than the left. Rostral body and anterior midbody of the corpus callosum were most frequently affected, mostly due to craniotomy with a transcallosal approach, ommaya reservoir placement, and ventriculostomy.

### Radiation doses to white matter structures

Table 1 summarizes the radiation dose to 51 white matter structures. The dose was highest to cerebral peduncle, corticospinal tract, fornix, pontine crossing tract, and anterior/posterior internal capsules, ranging from 37.9 to 49.9 CGE. Structures at the posterior region of the brain such as uncinate fasciculus and posterior thalamic radiation tended to receive the lowest doses (< 5 CGE).

### Radiation dose-effect on longitudinal changes in FA

In Fig. 2, the percentage changes of FA in all 51 white matter structures are plotted against their corresponding radiation doses. The three plots show FA changes at the three longitudinal times from baseline, depicting temporal evolution of the changes. Figure 2a shows FA reduction in most structures at 3 months from baseline (45 of 51). In this plot, the structures receiving higher doses (>40 CGE) did not show the largest FA reduction; that is, inter-structure dose effect was not apparent. The largest reductions were observed in bilateral cingulate gyrus (−5.6% for right and −6.4% for left) and the rostral body and anterior midbody of the corpus callosum (−4.8% and −4.9%, respectively). At 6 and 9 months (Figs. 2b and 2c), most structures appeared to be recovering from the reduced FA. For example, the FA changes in the rostral body of the corpus callosum were recovered to −3.6% and −3.7%, respectively (square symbol in Fig. 2). The LMEM analysis using all longitudinal data confirmed significant recovery in 29 structures. No structure showed progressive reduction.

Although inter-structure dose effect was not apparent, the LMEM analysis revealed an inter-patient dose effect— a greater reduction of FA in patients receiving a higher dose to a given structure— in 20 structures. These structures, marked with asterisks in Table 1, included left cerebral peduncle, body and splenium of the corpus callosum, and other structures with relatively large coefficients of variation of dose. Using right medial lemniscus as an example, Fig. 3(a) illustrates that the FA reduction is more pronounced in patients receiving higher doses (see supplementary figure for all the 20 structures). By contrast, structures without significant dose effect did not show such pronounced reduction as demonstrated by right anterior limb of internal capsule in Fig. 3(b).

### Accentuation of radiation dose-effect by surgical defects

The comparison of the test and control groups suggested that surgical defects in the corpus callosum accentuated the radiation dose-effect. The baseline age at treatment and dose to the surgery-affected or counterpart ROIs in the corpus callosum were not significantly different between the two groups (*t*-test, $P$=0.32 and 0.18, respectively). However, the baseline FA in the surgery-affected ROIs was 20% lower on average (P=0.0001) than that in the counterpart ROI. Three months after the proton therapy, the FA was further reduced by an average of −9.2% in surgery-affected ROIs. By contrast, the FA reduction was −1.3% in the counterpart ROI (Fig. 4a). The longitudinal analysis by LMEM confirmed that the FA reduction in the test group was significantly deeper and that the recovery was slower than that of the control group ($P$=0.0083). Other white matter structures not affected by surgery did not show differences in baseline and longitudinal FA values between the two groups (Fig. 4b) except for middle and superior cerebellar peduncles.

To illustrate an association with surgical approaches, the longitudinal DTI data of a group of patients who underwent transcallosal resection (n=6) were compared to those of a group who underwent transsphenoidal resection, which were subgroups of the test and control groups, respectively (Figs. 4c and 4d). The FA in the corpus callosum of the group receiving transcallosal resection showed a more pronounced reduction than did that of the transsphenoidal resection group, which showed minimal or no changes.

## Discussion

### Radiation dose-effect

The present study demonstrated that DTI can detect radiation-induced changes in cerebral white matter in patients with craniopharyngioma after post-operative proton therapy. The longitudinal DTI data indicated reductions in FA at 3 months after therapy, which was followed by a recovery in most white matter structures. The structures close to sellar and suprasellar regions tended to receive a higher dose, but the higher doses to these structures did not necessarily result in a greater FA reduction. However, we did observe inter-patient radiation dose-effect for a given structure. These results suggest that radiation dose-effect exists but the response may vary among structures or fiber tracts (15, 18). Confounding factors such as hemorrhage (23), hypercellularity (24), and surgical defects (the present study) could have contributed to the regional differences in observed responses.

### Comparison to previous DTI studies of photon therapy

Short-term changes in FA indices after treatment have been reported in previous studies on adult patients with brain tumor treated by photon therapy (9, 15, 16, 25). In contrast to our results, however, more severe and progressive changes were often observed. For instance, the FA in patients with brain metastases was reduced by 10% in body corpus callosum one month after whole-brain irradiation of 30 or 37.5 Gy (15). Another study (9) showed a linear trend of 20% reduction in FA in genu of the corpus callosum at 45 weeks after conformal radiation to patients with gliomas and other brain tumors. A possible cause of the discrepancy is the effect of concomitant chemotherapy (which our patients did not receive) in those studies because chemotherapy alone can alter normal white matter structures (26). This postulation is supported by a longitudinal study on patients not receiving chemotherapy (27), which showed a recovery or no further progression at 8 or 14 months after therapy and no change when the average dose was less than 45 Gy. Other possible causes of the discrepancy could be whole brain irradiation (15) as opposed to focal irradiation by proton therapy, higher dose to the target volume (range, 50–81 Gy) (9) than that in the present study (54 CGE), and differences in adult and pediatric patients.

### Effect of surgical defects and implications

The surgery-affected regions showed lower baseline FA, indicating compromised structural integrity before proton therapy. This compromise can be partly ascribed to Wallerian degeneration associated with the disconnected fiber tracts, as occurs in epilepsy patients receiving corpus callosotomy or temporal lobectomy (28–30). Wallerian degeneration may continue to develop along fiber tracts. However, our longitudinal data did not exhibit progressive FA reductions in regions closely connected to surgery- affected corpus callosum

(e.g., corona radiata), indicating that temporal development of surgery-associated Wallerian degeneration was not prevailing.

The present study suggested that the surgery-affected regions with compromised structural integrity may be more prone to radiation dose-effect than the other regions. The test of regions not affected by surgery did not indicate contributions by non-surgical factors. An interesting consequence was that surgical approaches could be associated with temporal changes of structural integrity: The structural integrity of the corpus callosum was not altered by using a transsphenoidal approach, but it was further compromised after proton therapy if a transcallosal approach was used. A notable implication of this finding is that surgical factors need to be considered in assessment of radiation dose-effect, which is particularly relevant to comparative studies of proton and photon treatments.

Neurocognitive and neurobehavioral dysfunctions are still among the primary concerns for complications in survivors of childhood craniopharyngioma (31–34). Previous studies have reported that post-therapeutic cognitive and behavioral outcomes were implicated by normal brain volume receiving a high radiation dose and various surgical factors such as CSF shunting, presence of ommaya reservoir, and extent of resection (32, 33). In line with previous findings, the current study found that radiation dose and surgery both affected the longitudinal behavior of white matter injury and recovery, thereby supporting further studies associating imaging changes with clinical outcomes.

## Limitations

Our results should be interpreted in light of a few limitations. Radiation effects may not fully manifest in DTI-derived indices within the relatively short post-therapeutic time studied (median of one year) (7). The present study was intended to inspect early image responses after proton therapy. Our findings will be confirmed as we continue long-term follow-up.

The comparison to previous DTI studies of photon therapy was limited due to the lack of DTI data corresponding to proton therapy of patients with craniopharyngioma. We could not determine association between dosimetric advantages in proton therapy and favorable structural integrity in white matter. In addition, relative biological effectiveness (RBE) of proton beams should be noted in interpreting the radiation dose-effect and comparison to photon therapy. Doses prescribed to our patients used spatially invariant RBE of 1.1 (35), following the current clinical practice. Although no clinical data clearly indicated that the use of this generic RBE was incorrect, uncertainty in RBE should be further investigated in future studies because of its dependency on a variety of factors including linear energy transfer, dose per fraction, and tissue type (36).

Due to the limited sample size in each subgroup of surgical approach, other potential confounding factors such as the time from surgery to proton therapy and the number of surgeries could not be further tested. The impact should be analyzed when a larger dataset becomes available.

## Conclusion

DTI data suggested the presence of short-term (3-month) effects of proton therapy on microstructures in the white matter. The subsequent data indicated that most white matter structures recovered. Surgical defects present at the time of proton therapy affected the integrity of cerebral white matter and appeared to accentuate the radiation dose-effect on its longitudinal behavior. This study supports consideration of pre-existing surgical defects and their locations in proton therapy planning and comparative studies of proton and photon beams.

## Supplementary Material

Refer to Web version on PubMed Central for supplementary material.

## Acknowledgments

Supported in part by funding from the American Lebanese Syrian Associated Charities (ALSAC)

## References

1. Kiehna EN, Merchant TE. Radiation therapy for pediatric craniopharyngioma. Neurosurg Focus. 2010; 28:E10.
2. Merchant TE, Kiehna EN, Sanford RA, et al. Craniopharyngioma: the St. Jude Children's Research Hospital experience 1984–2001. Int J Radiat Oncol Biol Phys. 2002; 53:533–542. [PubMed: 12062594]
3. Merchant TE, Kun LE, Hua CH, et al. Disease control after reduced volume conformal and intensity modulated radiation therapy for childhood craniopharyngioma. Int J Radiat Oncol Biol Phys. 2013; 85:e187–192. [PubMed: 23245282]
4. Bishop AJ, Greenfield B, Mahajan A, et al. Proton Beam Therapy Versus Conformal Photon Radiation Therapy for Childhood Craniopharyngioma: Multi-institutional Analysis of Outcomes, Cyst Dynamics, and Toxicity. Int J Radiat Oncol Biol Phys. 2014; 90:354–361. [PubMed: 25052561]
5. Winkfield KM, Linsenmeier C, Yock TI, et al. Surveillance of craniopharyngioma cyst growth in children treated with proton radiotherapy. Int J Radiat Oncol Biol Phys. 2009; 73:716–721. [PubMed: 18676089]
6. Steen RG, Koury BSM, Granja CI, et al. Effect of ionizing radiation on the human brain: white matter and gray matter T1 in pediatric brain tumor patients treated with conformal radiation therapy. Int J Radiat Oncol Biol Phys. 2001; 49:79–91. [PubMed: 11163500]
7. Dellani PR, Eder S, Gawehn J, et al. Late structural alterations of cerebral white matter in long-term survivors of childhood leukemia. J Magn Reson Imaging. 2008; 27:1250–1255. [PubMed: 18504742]
8. Khong PL, Kwong DL, Chan GC, et al. Diffusion-tensor imaging for the detection and quantification of treatment-induced white matter injury in children with medulloblastoma: a pilot study. AJNR Am J Neuroradiol. 2003; 24:734–740. [PubMed: 12695214]
9. Nagesh V, Tsien CI, Chenevert TL, et al. Radiation-induced changes in normal-appearing white matter in patients with cerebral tumors: a diffusion tensor imaging study. Int J Radiat Oncol Biol Phys. 2008; 70:1002–1010. [PubMed: 18313524]
10. Hua C, Merchant TE, Gajjar A, et al. Brain tumor therapy-induced changes in normal-appearing brainstem measured with longitudinal diffusion tensor imaging. Int J Radiat Oncol Biol Phys. 2012; 82:2047–2054. [PubMed: 21664060]

11. Aukema EJ, Caan MW, Oudhuis N, et al. White matter fractional anisotropy correlates with speed of processing and motor speed in young childhood cancer survivors. Int J Radiat Oncol Biol Phys. 2009; 74:837–843. [PubMed: 19117694]
12. Chapman CH, Nagesh V, Sundgren PC, et al. Diffusion tensor imaging of normal-appearing white matter as biomarker for radiation-induced late delayed cognitive decline. Int J Radiat Oncol Biol Phys. 2012; 82:2033–2040. [PubMed: 21570218]
13. Khong PL, Leung LH, Fung AS, et al. White matter anisotropy in post-treatment childhood cancer survivors: preliminary evidence of association with neurocognitive function. J Clin Oncol. 2006; 24:884–890. [PubMed: 16484697]
14. Palmer SL, Glass JO, Li Y, et al. White matter integrity is associated with cognitive processing in patients treated for a posterior fossa brain tumor. Neuro Oncol. 2012; 14:1185–1193. [PubMed: 22898373]
15. Chapman CH, Nazem-Zadeh M, Lee OE, et al. Regional variation in brain white matter diffusion index changes following chemoradiotherapy: a prospective study using tract-based spatial statistics. PLoS One. 2013; 8:e57768. [PubMed: 23469234]
16. Nazem-Zadeh MR, Chapman CH, Lawrence TL, et al. Radiation therapy effects on white matter fiber tracts of the limbic circuit. Med Phys. 2012; 39:5603–5613. [PubMed: 22957626]
17. Qiu D, Kwong DL, Chan GC, et al. Diffusion tensor magnetic resonance imaging finding of discrepant fractional anisotropy between the frontal and parietal lobes after whole-brain irradiation in childhood medulloblastoma survivors: reflection of regional white matter radiosensitivity? Int J Radiat Oncol Biol Phys. 2007; 69:846–851. [PubMed: 17544593]
18. Uh J, Merchant TE, Li Y, et al. Differences in brainstem fiber tract response to radiation: a longitudinal diffusion tensor imaging study. Int J Radiat Oncol Biol Phys. 2013; 86:292–297. [PubMed: 23474114]
19. Mori S, Oishi K, Jiang H, et al. Stereotaxic white matter atlas based on diffusion tensor imaging in an ICBM template. Neuroimage. 2008; 40:570–582. [PubMed: 18255316]
20. Witelson SF. Hand and sex differences in the isthmus and genu of the human corpus callosum. A postmortem morphological study. Brain. 1989; 112(Pt 3):799–835. [PubMed: 2731030]
21. Li L, Coles CD, Lynch ME, et al. Voxelwise and skeleton-based region of interest analysis of fetal alcohol syndrome and fetal alcohol spectrum disorders in young adults. Hum Brain Mapp. 2009; 30:3265–3274. [PubMed: 19278010]
22. Smith SM, Jenkinson M, Johansen-Berg H, et al. Tract-based spatial statistics: voxelwise analysis of multi-subject diffusion data. Neuroimage. 2006; 31:1487–1505. [PubMed: 16624579]
23. Qiu D, Leung LH, Kwong DL, et al. Mapping radiation dose distribution on the fractional anisotropy map: applications in the assessment of treatment-induced white matter injury. Neuroimage. 2006; 31:109–115. [PubMed: 16448821]
24. Ravn S, Holmberg M, Sorensen P, et al. Differences in supratentorial white matter diffusion after radiotherapy--new biomarker of normal brain tissue damage? Acta Oncol. 2013; 52:1314–1319. [PubMed: 23981047]
25. Chawla S, Wang S, Kim S, et al. Radiation Injury to the Normal Brain Measured by 3D-Echo-Planar Spectroscopic Imaging and Diffusion Tensor Imaging: Initial Experience. J Neuroimaging. 2013
26. Deprez S, Amant F, Yigit R, et al. Chemotherapy-induced structural changes in cerebral white matter and its correlation with impaired cognitive functioning in breast cancer patients. Hum Brain Mapp. 2011; 32:480–493. [PubMed: 20725909]
27. Haris M, Kumar S, Raj MK, et al. Serial diffusion tensor imaging to characterize radiation-induced changes in normal-appearing white matter following radiotherapy in patients with adult low-grade gliomas. Radiat Med. 2008; 26:140–150. [PubMed: 18683569]
28. Concha L, Gross DW, Wheatley BM, et al. Diffusion tensor imaging of time-dependent axonal and myelin degradation after corpus callosotomy in epilepsy patients. Neuroimage. 2006; 32:1090–1099. [PubMed: 16765064]
29. Liu M, Gross DW, Wheatley BM, et al. The acute phase of Wallerian degeneration: longitudinal diffusion tensor imaging of the fornix following temporal lobe surgery. Neuroimage. 2013; 74:128–139. [PubMed: 23396161]

30. McDonald CR, Hagler DJ Jr, Girard HM, et al. Changes in fiber tract integrity and visual fields after anterior temporal lobectomy. Neurology. 2010; 75:1631–1638. [PubMed: 20881271]

31. Di Pinto M, Conklin HM, Li C, et al. Learning and memory following conformal radiation therapy for pediatric craniopharyngioma and low-grade glioma. Int J Radiat Oncol Biol Phys. 2012; 84:e363–369. [PubMed: 22867897]

32. Dolson EP, Conklin HM, Li C, et al. Predicting behavioral problems in craniopharyngioma survivors after conformal radiation therapy. Pediatr Blood Cancer. 2009; 52:860–864. [PubMed: 19191345]

33. Merchant TE, Kiehna EN, Kun LE, et al. Phase II trial of conformal radiation therapy for pediatric patients with craniopharyngioma and correlation of surgical factors and radiation dosimetry with change in cognitive function. J Neurosurg. 2006; 104:94–102. [PubMed: 16506496]

34. Zada G, Kintz N, Pulido M, et al. Prevalence of neurobehavioral, social, and emotional dysfunction in patients treated for childhood craniopharyngioma: a systematic literature review. PLoS One. 2013; 8:e76562. [PubMed: 24223703]

35. Paganetti H, Niemierko A, Ancukiewicz M, et al. Relative biological effectiveness (RBE) values for proton beam therapy. Int J Radiat Oncol Biol Phys. 2002; 53:407–421. [PubMed: 12023146]

36. Paganetti H. Relative biological effectiveness (RBE) values for proton beam therapy. Variations as a function of biological endpoint, dose, and linear energy transfer. Phys Med Biol. 2014; 59:R419–472. [PubMed: 25361443]

## Summary

Longitudinal diffusion tensor imaging data of 51 patients with craniopharyngioma were analyzed to determine the effects of surgery and proton therapy on the microstructural integrity of cerebral white matter. The imaging data suggested short-term (3-month) effects of proton therapy followed by a recovery in most white matter structures. Surgical defects present at the time of proton therapy appeared to accentuate the radiation dose-effect.

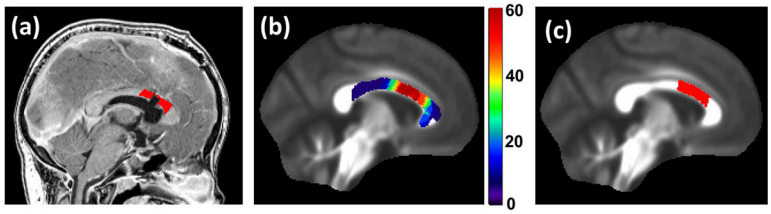


**Fig. 1.**

Regions of interest (ROIs) in the corpus callosum for testing the effect of surgical defects on the radiation dose-effect. (a) A representative surgery-affected ROI (colored red, within 10 mm in the standard brain space) overlaid on the T1-weighted MR image. (b) Percentage frequency of occupation by surgery-affected ROIs overlaid on an FA template. (c) The region most frequently occupied by surgery-affected ROIs; this region was used in the control group. The size of this counterpart ROI was made to be the same as the average size of the surgery-affected ROIs.

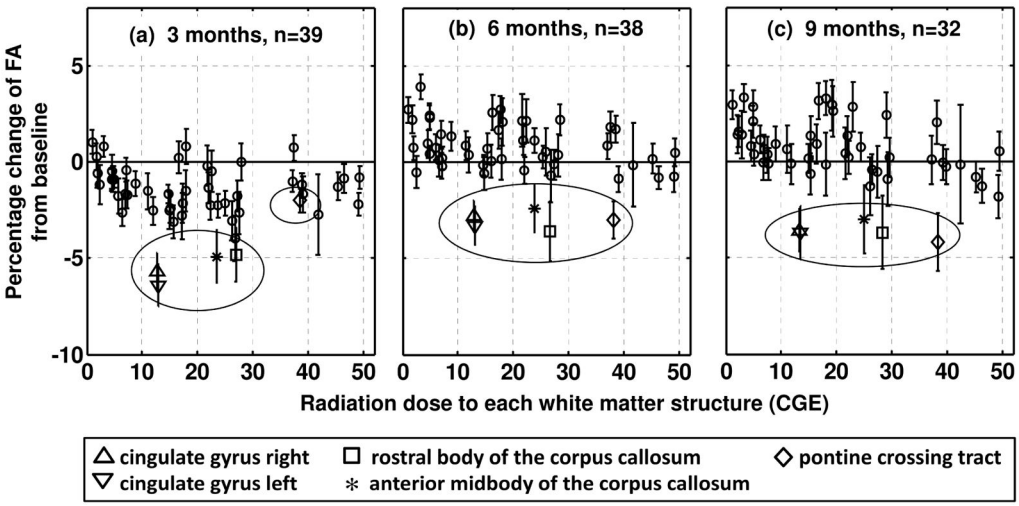


**Fig. 2.**

Average percentage change of FA in the 51 white matter structures plotted against the average dose. The three plots respectively correspond to different longitudinal times from baseline (3, 6, and 9 months). The structures showing persistent reductions (greater than 3%) at 9 months are presented by unique symbols and marked by a circle. The error bars represent standard error of the mean.

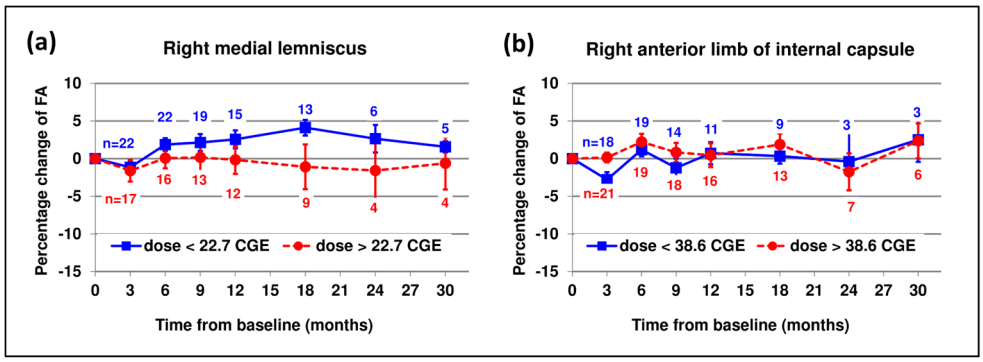


**Fig. 3.**

Radiation dose-effect in right medial lemniscus (a) in comparison with right anterior limb of internal capsule without significant dose effect (b). The FA changes of the patients receiving a dose higher than the average (circle with dotted line) are compared with those of the other patients (square with solid line). These plots are for illustration purposes only. The statistical analysis did not group the patients according to the dose. It should also be noted that the number of patients (n) differs at each longitudinal data point. The error bars represent standard error of the mean.

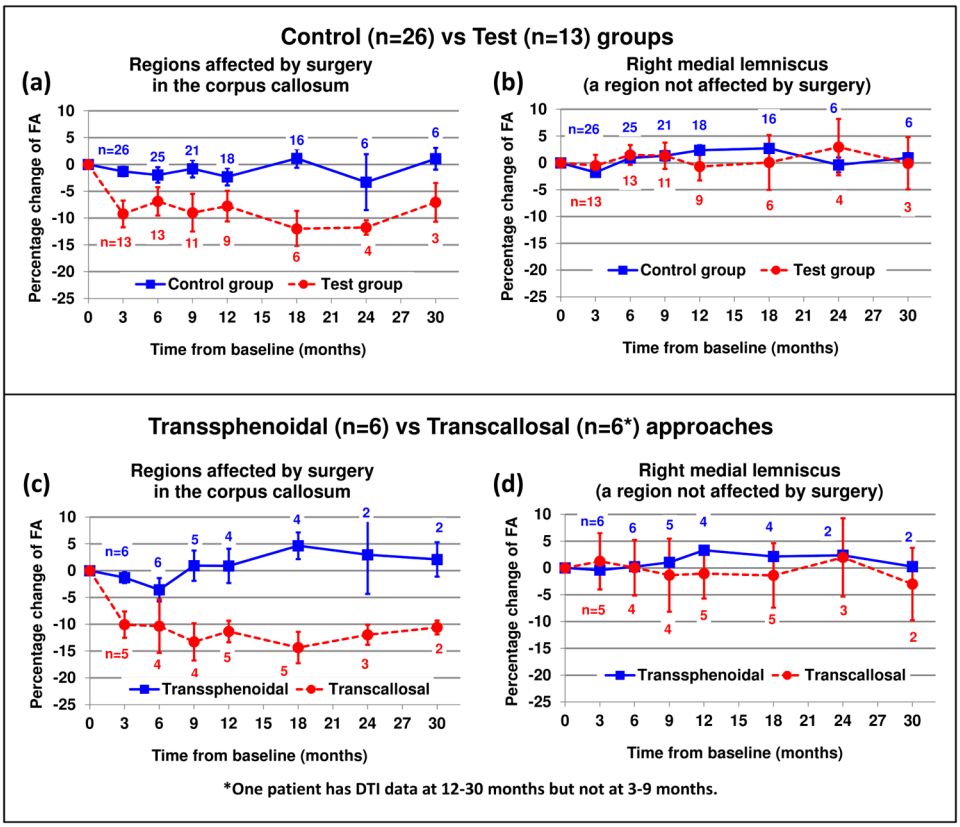


**Fig. 4.**

Effect of surgical defects on radiation dose-effect. (a) The surgery-affected ROI in patients of the test group underwent more reduction in FA than did the counterpart ROI in patients of the control group. (b) A region not affected by surgery (right medial lemniscus) did not show significant differences between the two groups. For illustration, the comparison was conducted again by using subgroups classified according to surgical approaches (c,d). The error bars represent standard error of the mean.

## Table 1

Average radiation doses to the major white matter structures defined by ICBM DTI-81 atlas (n=51).

| White matter structure | Dose in CGE (coefficient of variation) | | Surgical defects† | |
|---|---|---|---|---|
| | R | L | R | L |
| cerebral peduncle | 49.9 (0.13) | 49.9 (0.12)* | | |
| corticospinal tract | 45.8 (0.18) | 46.8 (0.18) | | |
| fornix | 42.1 (0.24) | | 4 | |
| pontine crossing tract | 39.1 (0.36) | | | |
| anterior limb of internal capsule | 38.6 (0.19) | 38.2 (0.18) | 1 | |
| posterior limb of internal capsule | 37.9 (0.23) | 37.9 (0.24) | 2 | |
| inferior fronto-occipital fasciculus | 27.7 (0.37) | 26.9 (0.40) | | |
| superior fronto-occipital fasciculus | 26.0 (0.33)* | 26.0 (0.32) | 2 | |
| genu of corpus callosum | 25.5 (0.49) | | 4 | |
| rostral body of corpus callosum | 25.2 (0.45)* | | 12 | |
| external capsule | 23.8 (0.31) | 24.5 (0.33) | 1 | |
| cingulum (hippocampus) | 23.0 (0.57) | 23.1 (0.59)* | | |
| anterior midbody of corpus callosum | 22.8 (0.39)* | | 10 | |
| medial lemniscus | 22.7 (0.78)* | 22.4 (0.79)* | | |
| superior cerebellar peduncle | 17.6 (0.74) | 18.6 (0.73) | | |
| posterior midbody of corpus callosum | 17.9 (0.51)* | | 1 | |
| anterior corona radiata | 16.2 (0.65) | 15.8 (0.66) | 5 | 1 |
| superior corona radiata | 15.4 (0.50) | 15.7 (0.46) | 8 | 1 |
| middle cerebellar peduncle | 14.9 (0.61) | | | |
| fornix/stria terminalis | 13.3 (0.88) | 15.3 (0.84)* | | |
| cingulum (cingulate gyrus) | 12.7 (0.55)* | 13.2 (0.53) | 3 | 1 |
| isthmus of corpus callosum | 12.3 (0.86)* | | | |
| retrolenticular part of internal capsule | 8.2 (1.10)* | 9.3 (1.16) | | |
| inferior cerebellar peduncle | 7.3 (1.76)* | 7.2 (1.86)* | | |
| sagittal stratum | 5.1 (1.25) | 6.7 (1.46) | | |
| splenium of corpus callosum | 5.8 (1.50)* | | | |
| superior longitudinal fasciculus | 5.3 (0.83) | 6.0 (0.97)* | 1 | |
| posterior corona radiata | 3.7 (1.70) | 5.1 (1.45)* | | |
| uncinate fasciculus | 1.8 (3.16)* | 2.7 (2.49) | | |
| posterior thalamic radiation | 0.9 (3.78)* | 1.9 (2.72)* | | |

*Abbreviations:* CGE=cobalt gray equivalent; R=right; L=left.

*Structures showing significant radiation dose effect.

†The number of patients presenting surgical corridors or catheter tracks.